

Similarity of particle systems using an invariant root mean square deviation measure

Johannes Bulin^{1,*} and Jan Hamaekers^{1,2}

¹Department of Virtual Material Design, Fraunhofer Institute for Algorithms and Scientific Computing, Schloss Birlinghoven, 53757 Sankt Augustin, Germany

²Fraunhofer Center for Machine Learning, Schloss Birlinghoven, 53757 Sankt Augustin, Germany

*Corresponding author: johannes.bulin@scai.fraunhofer.de

Determining whether two particle systems are similar is a common problem in particle simulations. When the comparison should be invariant under permutations, orthogonal transformations, and translations of the systems, special techniques are needed. We present an algorithm that can test particle systems of finite size for similarity and, if they are similar, can find the optimal alignment between them. Our approach is based on an invariant version of the root mean square deviation (RMSD) measure and is capable of finding the globally optimal solution in $O(n^3)$ operations where n is the number of three-dimensional particles.

1 Introduction

The comparison of particle systems is a subproblem that occurs frequently in many interesting problems ranging from the analysis of certain substructures to different machine learning approaches. One particular use case is databases that store particle systems and corresponding properties. In many cases, some of these properties such as the potential energy are invariant under particle index permutations, translations, and orthogonal transformations of the system. Other properties, such as forces, can be readily transferred from one system to a transformed instance of itself if the corresponding transformations are known. To exploit these invariances, it is necessary to check two particle systems for

similarity up to these invariances and – if the two systems are similar – to obtain the corresponding transformations.

Some attempts have been made that use this idea. In [1], a database was presented that stores atomic neighbourhoods and corresponding forces. Instead of forces, the databases in [2] and [3] hold local transition information that is then used in a localised kinetic Monte Carlo algorithm. Depending on the choice of the comparison procedure, the problem of false positives and negatives may occur: false positives (two systems are designated as similar, despite not being so) may have catastrophic consequences, as incorrect properties can be attributed to a system. False negatives (two similar systems are not recognised as such) may cause a waste of computational time, as properties that already exist in the database must be recomputed. The comparison techniques in [2] and [3] may cause false positives as the comparison is done on a reduced representation of a system. In [1], an approximate algorithm was used to check for similarity that can result in false negatives.

To avoid false positives/negatives we introduce a comparison procedure that is based on an invariant version of the root mean square deviation measure (RMSD). It is able to check particle systems for similarity and – if two systems are similar – can also calculate the transformations that align one system to the other. We also prove that our algorithm finds the globally optimal solutions in no more than $O(n^3)$ operations where n is the number of three-dimensional particles.

2 The invariant RMSD

Before introducing the invariant RMSD, we need a mathematical definition of a *particle system*. In this work, we define a particle system $S = (\mathbf{x}, \mathbf{e})$ by its n d -dimensional coordinates $\mathbf{x} = (x_1, \dots, x_n)$ where $x_i \in \mathbb{R}^d$ and corresponding particle elements $\mathbf{e} = (e_1, \dots, e_n)$ with $e_i \in \mathbb{Z}$. This allows us to represent molecules as well as atomic neighbourhoods.

For two particle systems $S = (\mathbf{x}, \mathbf{e})$ and $\tilde{S} = (\tilde{\mathbf{x}}, \tilde{\mathbf{e}})$ the classical RMSD is defined as

$$RMSD(S, \tilde{S}) = \begin{cases} \infty, & \exists i : e_i \neq \tilde{e}_i \\ \sqrt{\sum_{i=1}^n \|x_i - \tilde{x}_i\|_2^2}, & \text{otherwise.} \end{cases} \quad (1)$$

Similar to the work in [4, 1, 5] we obtain invariance under orthogonal transformations, translations, and permutations by minimising over all such transformations. We call the resulting distance measure the *invariant RMSD (IRMSD)*:

$$IRMSD(S, \tilde{S}) = \min_{\pi \in \mathbb{S}_n, \mathbf{R} \in \mathbb{O}_d, \mathbf{T} \in \mathbb{R}^d} \begin{cases} \infty, & \exists i : \tilde{e}_{\pi_i} \neq e_i \\ \sqrt{\|x_i - \mathbf{R}\tilde{x}_{\pi_i} - \mathbf{T}\|_2^2}, & \text{otherwise.} \end{cases} \quad (2)$$

Here, \mathbb{O}_d is the set of all $d \times d$ orthogonal matrices while \mathbb{S}_n is the set of all permutations of length n .

The *IRMSD* has a number of properties that makes it suitable for comparing particle systems. $IRMSD(S, \tilde{S}) = 0$ if and only if S and \tilde{S} are equal up to the mentioned

transformations. Thus, if we define two systems as similar if $IRMSD(S, \tilde{S}) = 0$ we will not have any problems with false positives or negatives. $IRMSD$ is also continuous with respect to the particle coordinates and – if the elements are ignored – fulfils all properties of a pseudometric on $\mathbb{R}^{n \times d}$.

Due to the presence of numerical inaccuracies and different types of noise, checking for $IRMSD(S, \tilde{S}) = 0$ will in most cases not be useful. For practical purposes, we consider two particle systems S and \tilde{S} as similar if

$$IRMSD(S, \tilde{S}) \leq \epsilon \tag{3}$$

for some tolerance ϵ .

3 Calculating the invariant RMSD

For arbitrary particle systems S and \tilde{S} , calculating $IRMSD(S, \tilde{S})$ is an NP-hard problem [4, 5]. Nevertheless, several ways to calculate or approximate it have been proposed. One class of algorithms calculates only approximations to $IRMSD(S, \tilde{S})$. This includes the algorithms in [4, 1] but also various approaches in computer vision [6, 7] where point sets are compared, instead of particle systems. As only approximations to the $IRMSD$ are calculated, this class of algorithms may cause false positives/negatives when comparing particle systems.

A second class of algorithms, including the methods given in [5, 8, 9], is able to calculate the exact value $IRMSD(S, \tilde{S})$ if run long enough (which may scale exponentially with the number of particles). For many particle systems, some of these algorithms can nevertheless calculate $IRMSD(S, \tilde{S})$ rapidly. For other systems, especially highly symmetric ones, they can be prohibitively slow (see evaluation section).

In our setting it is sufficient to check whether $IRMSD(S, \tilde{S}) \leq \epsilon$; only in this case must we calculate the exact value of $IRMSD$ and the corresponding transformations. In the context of particle simulations, we can also assume that the distance between two particles is bounded from below by a minimum particle distance μ . This can be motivated by the strong repulsive forces that act between atoms that are close to each other. Using this property, we introduce a new algorithm for this special kind of problem. It can determine whether the inequality in equation 3 holds true or not and, if so, is able to calculate the exact value $IRMSD(S, \tilde{S})$ and the corresponding optimal transformations.

In the following, if we compare two particle systems $S = (\mathbf{x}, \mathbf{e})$ and $\tilde{S} = (\tilde{\mathbf{x}}, \tilde{\mathbf{e}})$ we assume that at least one of them has full rank. In this context that means that either \mathbf{x} or $\tilde{\mathbf{x}}$ contain d linearly independent points. If this is not the case, one can reduce the dimensionality of the points (for example by using PCA) and calculate the $IRMSD$ for the reduced coordinates.

For notational simplicity, we skip the calculation of the optimal translations in equation 2. This can be done by pre-shifting both particle systems such that the centroids of the coordinates are both at the origin. In this case, the optimal translation is always the 0-vector.

Algorithm 1 Check whether $IRMSD(S, \tilde{S}) \leq \epsilon$.

Require: Two particle systems $S = (\mathbf{x}, \mathbf{e})$, $\tilde{S} = (\tilde{\mathbf{x}}, \tilde{\mathbf{e}})$.

Require: $\tilde{\mathbf{x}}$ must have full rank.

Require: $\epsilon < \frac{\mu}{2\sqrt{1+4d}}$.

Require: $\|x_i - x_j\|_2 \geq \mu \forall i \neq j$.

Require: $\|\tilde{x}_i - \tilde{x}_j\|_2 \geq \mu \forall i \neq j$.

```

1:  $g^* = \infty$ 
2:  $\mathbf{R}^* = I$ 
3:  $\pi^* = id$ 
4: if  $sort(e) \neq sort(\tilde{e})$  then
5:   return  $IRMSD(S, \tilde{S}) \not\leq \epsilon$ 
6: end if
7: Choose the  $d$  indices  $j_1, \dots, j_d$  that maximise the absolute value of the determinant
   of  $[\tilde{x}_{j_1}, \dots, \tilde{x}_{j_d}]$ .
8: for all  $i_1, \dots, i_d : e_{i_k} = \tilde{e}_{j_k} (k = 1, \dots, d)$  do
9:    $\mathbf{R} = \arg \min_{\mathbf{R} \in \mathbb{O}_d} \sum_{k=1}^d \|x_{i_k} - \mathbf{R}\tilde{x}_{j_k}\|_2^2$ 
10:   $g = \sum_{k=1}^d \|x_{i_k} - \mathbf{R}\tilde{x}_{j_k}\|_2^2$ 
11:  if  $g > \epsilon^2$  then
12:    continue
13:  end if
14:  Set  $\pi \in \mathbb{S}_n$  s.t.  $\pi_{i_k} = j_k (\forall k \in \{1, \dots, d\})$ ,  $\pi_k = \arg \min_{l: e_k = \tilde{e}_l} \|x_k - \mathbf{R}\tilde{x}_l\|_2$ 
   ( $\forall k \notin \{i_1, \dots, i_d\}$ )
15:   $\tilde{\mathbf{R}} = \arg \min_{\mathbf{R} \in \mathbb{O}_d} \sum_{k=1}^n \|x_k - \mathbf{R}\tilde{x}_{\pi_k}\|_2^2$ 
16:   $\tilde{g} = \sqrt{\sum_{k=1}^n \|x_k - \tilde{\mathbf{R}}\tilde{x}_{\pi_k}\|_2^2}$ 
17:  if  $\tilde{g} \leq g^*$  then
18:     $g^* = \tilde{g}$ 
19:     $\mathbf{R}^* = \tilde{\mathbf{R}}$ 
20:     $\pi^* = \pi$ 
21:  end if
22: end for
23: if  $g^* \leq \epsilon$  then return  $g^*, \mathbf{R}^*, \pi^*$ 
24: else
25:   return  $IRMSD(S, \tilde{S}) \not\leq \epsilon$ 
26: end if

```

Our new algorithm (see algorithm 1) is essentially a three-step procedure. In the first step (line 7), d maximally linearly independent particles are chosen from the first system S , meaning that the corresponding particle coordinates maximise the determinant of the matrix that they form. Afterwards, all length- d combinations of particles in the other system \tilde{S} are determined such that these particles can be mapped onto the previously chosen d particles in the other system, using only an orthogonal transformation (up

to the tolerance ϵ). If $IRMSD(S, \tilde{S}) \leq \epsilon$ and $\epsilon < \frac{\mu}{2\sqrt{1+4d}}$, one of these orthogonal transformations (line 9) is close enough to the globally optimal orthogonal transformation such that it can be used to determine the globally optimal permutation (see theorem 3 in the appendix). Thus, in one of the for-loop cycles algorithm 1 will calculate the globally optimal permutation π^* and thus the corresponding globally optimal orthogonal transformation in line 15. All necessary proofs can be found in the appendix.

4 Time complexity

To determine the time complexity of algorithm 1, its three key components must be analysed: the cost of calculating the indices in line 7, the cost of the lines 9-10, and the cost of the lines 14-16.

We begin with line 7. The d indices that maximise the determinant can be calculated by a brute-force search over all $\binom{n}{d}$ combinations. For each combination the determinant of the corresponding matrix must be calculated, which requires $O(d^3)$ operations. Combined, the time complexity of line 7 is $O(n^d d^3)$.

Calculating \mathbf{R} in line 9 can be done by using the Kabsch algorithm [10], which needs $O(d^3)$ operations. The subsequent calculation of g in line 10 also has time complexity $O(d^3)$. As these two lines may be called up to $\binom{n}{d}$ many times, they contribute $O(n^d d^3)$ operations to the total complexity.

It can be shown that there are no more than $2.415^d \binom{n}{d-1}$ index combinations i_1, \dots, i_d such that g in line 10 fulfils $g \leq \epsilon^2$ (see theorem 5 in the appendix). Thus line 14 and subsequent parts of the code are called no more than $O(2.415^d n^{d-1})$ times. The permutation π in line 14 can be calculated by a cell based approach in $O(3^d dn)$ operations [11]. Both $\tilde{\mathbf{R}}$ and \tilde{g} in lines 9 and 16 can be calculated in $O(nd^2 + d^3)$ operations, once again using the Kabsch algorithm. Therefore, the total contributions of lines 14 - 16 to the time complexity is of order $O(2.415^d n^{d-1} (3^d dn + nd^2 + d^3)) = O(7.245^d n^d d)$. Thus for the fixed ‘‘standard’’ dimensions $d = 2$ and $d = 3$, the algorithm has complexity $O(n^2)$ and $O(n^3)$, respectively.

5 Evaluation

To verify the theoretical results we have implemented our algorithm for three-dimensional particles as an extension module for the QuantumATK software package [12, 13].

Four different datasets were used for testing. The first dataset (*silicon dataset*) was derived from the database of silicon configurations in [14, 15]. For each configuration in the database we calculated the atomic neighbourhoods of radius 6\AA of all particles in this configuration. Using these neighbourhoods, one million neighbourhood pairs (S_i, \tilde{S}_i) were randomly chosen such that S_i and \tilde{S}_i have the same number of particles.

The next dataset (*C720 dataset*) was generated using the C₇₂₀ fullerene molecule. The coordinates $\mathbf{c} = (c_1, \dots, c_n)$ and elements $\mathbf{e} = (e_1, \dots, e_n)$ ($n = 720$) of this molecule

were taken and 1000 pairs (S_i, \tilde{S}_i) defined by

$$\begin{aligned} S_i &= (\mathbf{R}^{(i)} \mathbf{c}_{\pi^{(i)}}, \mathbf{e}_{\pi^{(i)}}) \\ \tilde{S}_i &= \left(\tilde{\mathbf{R}}^{(i)} \mathbf{c}_{\tilde{\pi}^{(i)}} + \frac{\tau^{(i)}}{\|\tau^{(i)}\|_F} \rho^{(i)}, \mathbf{e}_{\tilde{\pi}^{(i)}} \right) \end{aligned} \quad (4)$$

were generated. $\mathbf{R}^{(i)}$ and $\tilde{\mathbf{R}}^{(i)}$ are random rotation matrices whereas $\pi^{(i)}$ and $\tilde{\pi}^{(i)}$ are random permutations. Additional noise was added in the form of $\tau^{(i)}$ which was drawn from the $3n$ -dimensional multivariate standard normal distribution $\mathcal{N}(0, I)$. This noise was scaled by $\rho^{(i)} / \|\tau^{(i)}\|_2$ where $\rho^{(i)}$ is exponentially distributed with parameter $\lambda = 3$. This ensures that the magnitude of the noise

$$\left\| \frac{\tau^{(i)}}{\|\tau^{(i)}\|_F} \rho^{(i)} \right\|_F = \rho^{(i)} \quad (5)$$

varies from zero noise ($\rho^{(i)} = 0$) to very noisy ($\rho^{(i)}$ large).

The *diamond dataset* was created in a similar way. For different cutoff radii r we calculated the atomic neighbourhood of some particle in a perfect diamond crystal (the choice of the particle is unimportant as all neighbourhoods are equal). Using the coordinates $\mathbf{c}^{(r)}$ and elements $\mathbf{e}^{(r)}$ of this neighbourhood we generated 1000 pairs $(S_i^{(r)}, \tilde{S}_i^{(r)})$ in the same way as in equation 4.

Finally the *spherical dataset* was created to investigate the behaviour of the algorithm over systems of different sizes. For different numbers of particles n we distributed n points almost uniformly on the unit sphere using generalised spiral points from [16]. The sphere was then scaled such that the minimal distance between two points became 2\AA . These coordinates $\mathbf{c}^{(n)}$ were then used to build 100 particle system pairs $(S_i^{(n)}, \tilde{S}_i^{(n)})$ by the application of random orthogonal transformations and permutations (no noise was used). For all particles, the same elements were used.

As reference algorithms we chose Go-ICP [8, 17] and Go-Permdist [9, 18]. These two algorithms are branch-and-bound based and calculate the optimal solution. In both algorithm we have disabled the calculation of the optimal translation as it caused Go-ICP to become much slower (the translation search in Go-ICP is expensive as it also supports registration problems without one-to-one correspondences which is harder). As mentioned earlier, it is also easy to decouple the calculation of the optimal translation from finding the optimal permutation and orthogonal transformation.

We also modified the code such that both algorithm will stop their calculations if the lower bounds in the branch-and-bound section become larger than the tolerance ϵ . As we only need to check for similarity, it is not necessary to calculate the exact value $IRMSD(S, \tilde{S})$ once it has been established that $IRMSD(S, \tilde{S}) > \epsilon$. For both algorithm we stopped the calculation as soon as the difference between the lower and upper bounds became smaller than 10^{-2} .

During our calculations we found a small mistake in the calculation of the lower bounds in the Go-Permdist algorithm that caused false negatives in a few cases. We thus modified

the Go-Permdist algorithm such that it used our corrected lower bounds. The corrected terms can be found in the appendix.

5.1 Accuracy

We began by testing the accuracy of the algorithms. To do this, we applied the three algorithms to all particle system pairs in the three datasets and compared the results for different tolerances $\epsilon < \frac{\mu}{2\sqrt{1+4d}}$. As Go-ICP and Go-Permdist optimise only over all rotations and not over all orthogonal transformations (which also includes reflections), we encountered a few cases where our algorithm calculated smaller *IRMSD* values. This was expected and occurred only when the optimal orthogonal transformation was not a rotation matrix. In the subsequent performance analysis we simply excluded these cases as not relevant.

Otherwise, we could not detect any differences between the three algorithms in terms of the results that they calculated. The *IRMSD* values that the three algorithms computed never differed by more than 10^{-2} , which was the chosen stopping criterion for Go-ICP and Go-Permdist.

When testing the unfixed Go-Permdist algorithm we encountered some false negatives where the algorithm wrongly determined that $IRMSD(S, \tilde{S}) > \epsilon$. The corrected Go-Permdist algorithm did not suffer from such problems.

5.2 General Performance

Next, we investigate the performance of our algorithm in terms of computational efficiency. To do this we measured the wall time that was necessary to compare each pair in our three datasets. All the tests were run on a single core of an Intel Xeon Gold 5118 processor using the tolerance $\epsilon = 0.2\text{\AA}$.

Figure 1 shows the distribution of the runtimes on the silicon dataset. We observe that our algorithm is on average about four times faster than Go-Permdist and ten times faster than Go-ICP. Interestingly, Go-ICP and Go-Permdist show a much higher variation in runtime. Whereas our algorithm never needs more than 0.07s for a comparison, this value is 2.3s for Go-ICP and 371.8s for the (fixed) Go-Permdist algorithm. We investigated this behaviour and observed that all three algorithms are slowest when the particle systems under investigation are highly symmetric. We note that our algorithm is much faster than Go-ICP and Go-Permdist in these cases. In the silicon dataset this occurred when atomic neighbourhoods with (almost) perfect crystal structure were encountered. By contrast, all three algorithms were very fast over particle systems with low symmetry such as linear chains of atoms.

We turn now to the C720 dataset. The C₇₂₀ fullerene is a highly symmetric molecule, so if our initial observations hold true, we might expect relatively slow calculations. As shown in figure 2 this seems to be the case. Our algorithm is much faster here than the two other algorithms. Go-ICP takes on average about 50 times more computational time, for Go-Permdist this figure increases to 500. Once again, the runtimes of Go-ICP and Go-Permdist span several orders of magnitude. Here, this behaviour cannot be

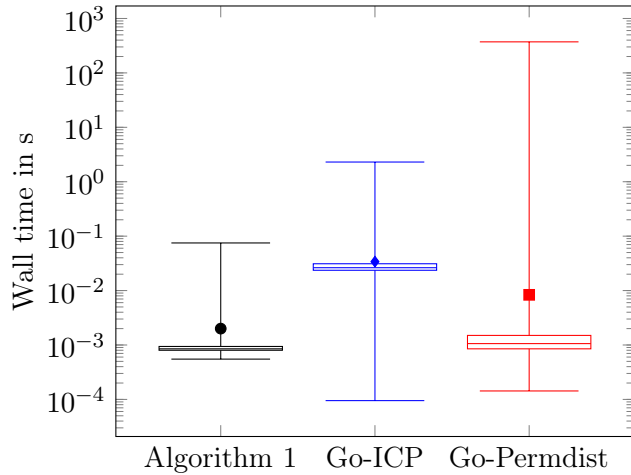


Figure 1: Distribution of the wall times in the silicon dataset. The lines show (starting from below) the 0% (minimum), 25%, 50% (median), 75% and 100% (maximum) percentile of the wall times. The mean runtime is represented by the single point.

explained by the variance in symmetry as all systems are (slightly perturbed) symmetric C_{720} molecules. However, we observed that Go-ICP and Go-Permdist can be very fast in two cases: first, when the optimal orthogonal transformation is close to the identity matrix and second, if a large amount of noise was added to the one of the particle systems.

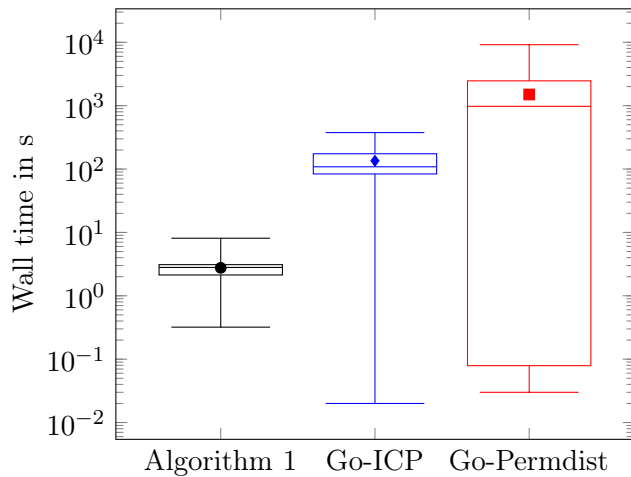


Figure 2: Distribution of the wall times in the C720 dataset.

We also ran our tests on the diamond dataset, choosing the cutoff radius $r = 6\text{\AA}$.

Similar to the C720 dataset, the diamond dataset contains highly symmetric particle systems. Unsurprisingly, the runtime plot in figure 3 looks similar to the corresponding figure for the C720 dataset. The runtimes are lower on average, which can be explained by the lower number of particles (159) per particle system compared to the C720 dataset (720).

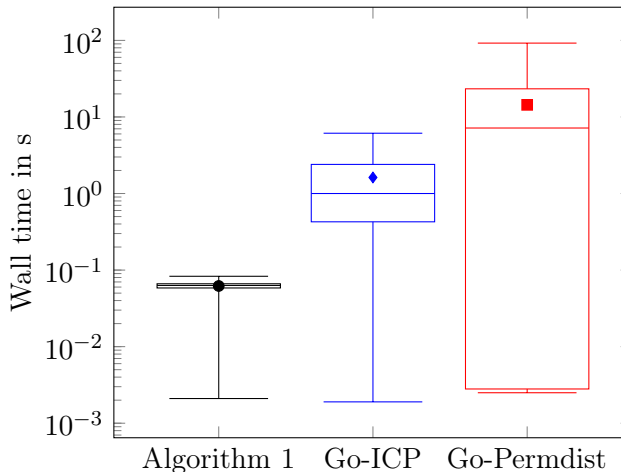


Figure 3: Distribution of the wall times in the diamond dataset ($r = 6\text{\AA}$).

5.3 Scaling

To test the scaling of the algorithms with respect to the size of the particle system, we used different cutoff radii in the diamond dataset to create systems of different sizes. Again setting $\epsilon = 0.2\text{\AA}$ we looked at the worst-case runtimes as shown in figure 4.

For all tested numbers of particles, the worst-case runtimes of our algorithm are much lower than those of the two reference algorithms, although the gap between Go-ICP and algorithm 1 seems to narrow for large numbers of particles. Unexpectedly, the run times of our algorithm seem to scale as $O(n^2)$ with the number of particles despite the fact that all particles are three-dimensional. This behaviour can be explained by the setup of the diamond dataset. To create the particle systems in this dataset, atomic neighbourhoods in a perfect diamond crystal were used. Due to the structure of a diamond crystal, the particles in such a neighbourhood are arranged in shells around the central particle of the neighbourhood. This shell-type structure reduces the number of possible permutations, as only particles with similar distances to the central particle may be matched to each other.

In the spherical dataset all particles in a particle system lie on the surface of some sphere, thus there exists only a single shell. When we use our algorithm on this dataset, we can actually see the $O(n^3)$ scaling that we expected in the beginning (see figure 5). Go-ICP and Go-Permdist also seem to scale cubically with the number of particles but

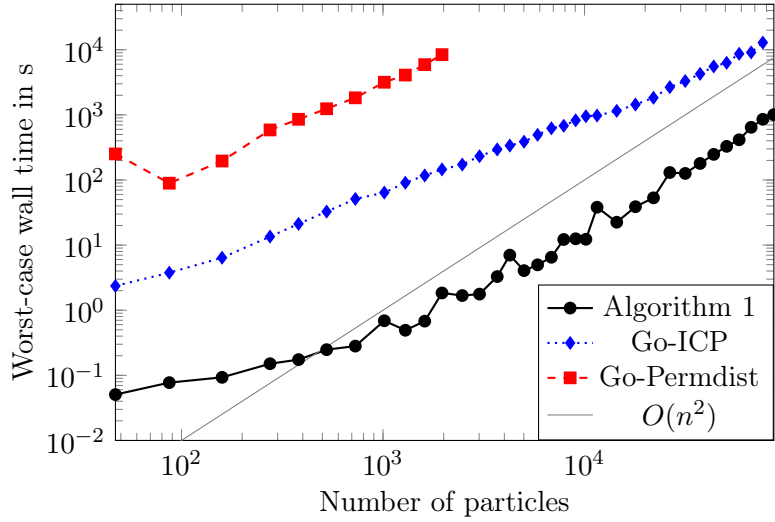


Figure 4: Worst-case wall times for the diamond example.

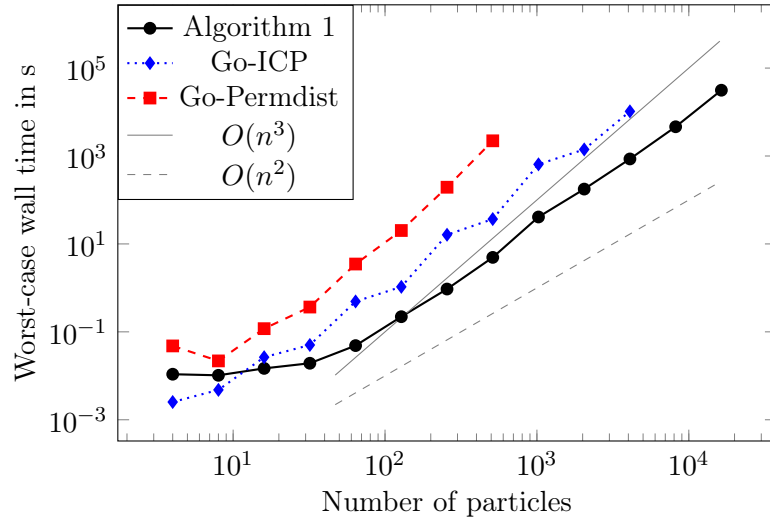


Figure 5: Worst-case wall times for the sphere example.

are much slower than algorithm 1, except for very small systems.

6 Conclusion

We have developed an algorithm that can be used to check particle systems for similarity and align them if they are similar. On average, our algorithm is faster than both Go-ICP

and Go-Permdist, in some cases by several orders of magnitude.

Compared to Go-ICP and Go-Permdist our algorithm is limited by the upper bound for the allowed tolerance ϵ and can thus be used only in some cases. While we do not think that this will cause problems when used in a database context as explained in the introduction, it might be worthwhile to extend algorithm 1 such that it resorts to some form of branch-and-bound-style permutation search if the tolerance ϵ is larger than the upper bound $\frac{\mu}{2\sqrt{1+4d}}$.

In this work we have presented only a comparison approach for particle systems. To build a database of particle systems, additional work is needed to design a database structure that supports the efficient querying of particle systems.

Appendix

6.1 Proofs

The first proof shows the consequences of choosing the indices j_1, \dots, j_d in algorithm 1:

Theorem 1. *Let $\mathbf{y} = (y_1, \dots, y_n)$ be n d -dimensional points ($y_i \in \mathbb{R}^d$) and assume that the matrix $[y_1 \dots y_n] \in \mathbb{R}^{d \times n}$ has full (column) rank d . Let j_1, \dots, j_d be the d indices that maximise*

$$\max_{j_1, \dots, j_d} \left| \det \left(\begin{bmatrix} | & & | \\ y_{j_1} & \dots & y_{j_d} \\ | & & | \end{bmatrix} \right) \right|. \quad (6)$$

Then each point y_i can be written as

$$y_i = \begin{bmatrix} | & & | \\ y_{j_1} & \dots & y_{j_d} \\ | & & | \end{bmatrix} v_i \quad (7)$$

where $v_i \in \mathbb{R}^d$ fulfils

$$\|v_i\|_\infty \leq 1. \quad (8)$$

We note that this theorem has already been stated in [19] though without an explicit proof.

Proof. As the matrix $[y_1 \dots y_n]$ is assumed to have full rank, the determinant in equation 6 is nonzero and therefore the matrix

$$\tilde{\mathbf{Y}} = \begin{bmatrix} | & & | \\ y_{j_1} & \dots & y_{j_d} \\ | & & | \end{bmatrix} \quad (9)$$

is invertible. We set $v_i = \tilde{\mathbf{Y}}^{-1} y_i$ for all indices i and show that it fulfils $\|v_i\|_\infty \leq 1$. Using Cramer's rule, the k -th component of v_i is given by

$$(v_i)_k = (\tilde{\mathbf{Y}}^{-1} y_i)_k = \frac{\det \tilde{\mathbf{Y}}^{(i,k)}}{\det \tilde{\mathbf{Y}}}. \quad (10)$$

$\tilde{\mathbf{Y}}^{(i,k)}$ is the matrix that arises when the k -th column of $\tilde{\mathbf{Y}}$ is replaced by y_i . As $|\det \tilde{\mathbf{Y}}| \geq |\det \tilde{\mathbf{Y}}^{(i,k)}|$ by definition, we finally obtain

$$\|v_i\|_\infty = \max_k |(v_i)_k| = \max_k \left| \frac{\det \tilde{\mathbf{Y}}^{(i,k)}}{\det \tilde{\mathbf{Y}}} \right| \leq 1. \quad (11)$$

□

Theorem 2. Let $\mathbf{x} = (x_1, \dots, x_n)$ and $\mathbf{y} = (y_1, \dots, y_n)$ be n d -dimensional points each ($x_i \in \mathbb{R}^d$ and $y_i \in \mathbb{R}^d$). Assume that the y_1, \dots, y_n fulfill the assumptions in theorem 1 and let j_1, \dots, j_d be the corresponding indices that maximise equation 6. Also let i_1, \dots, i_d be d distinct indices, $\mathbf{R} \in \mathbb{O}_d$ and $\tilde{\mathbf{R}} \in \mathbb{O}_d$ arbitrary orthogonal transformations and $\pi \in \mathbb{S}_n$ an arbitrary permutation that fulfils $\pi_{i_k} = j_k$ ($\forall k = 1, \dots, d$).

Then for any $l = 1, \dots, n$, it holds that

$$\|(\mathbf{R} - \tilde{\mathbf{R}})y_l\|_2 \leq \sqrt{d}(\tilde{\delta} + \delta), \quad (12)$$

where

$$\delta = \sqrt{\sum_{k=1}^d \|x_{i_k} - \mathbf{R}y_{\pi_{i_k}}\|_2^2} \quad (13)$$

$$\tilde{\delta} = \sqrt{\sum_{k=1}^d \|x_{i_k} - \tilde{\mathbf{R}}y_{\pi_{i_k}}\|_2^2}. \quad (14)$$

Proof. Using the inequality $\sum_i^d |a_i| \leq \sqrt{d \sum_i^d a_i^2}$ we obtain

$$\begin{aligned} \sum_{k=1}^d \|(\mathbf{R} - \tilde{\mathbf{R}})y_{j_k}\|_2 &= \sum_{k=1}^d \|(\mathbf{R} - \tilde{\mathbf{R}})y_{\pi_{i_k}}\|_2 \\ &= \sum_{k=1}^d \|(\mathbf{R} - \tilde{\mathbf{R}})y_{\pi_{i_k}} + x_{i_k} - x_{i_k}\|_2 \\ &\leq \sum_{k=1}^d \|x_{i_k} - \tilde{\mathbf{R}}y_{\pi_{i_k}}\|_2 + \|x_{i_k} - \mathbf{R}y_{\pi_{i_k}}\|_2 \\ &\leq \sqrt{d \sum_{k=1}^d \|x_{i_k} - \tilde{\mathbf{R}}y_{\pi_{i_k}}\|_2^2} \\ &\quad + \sqrt{d \sum_{k=1}^d \|x_{i_k} - \mathbf{R}y_{\pi_{i_k}}\|_2^2} \\ &\leq \sqrt{d}(\tilde{\delta} + \delta). \end{aligned}$$

Using theorem 1 we can write every y_l as

$$y_l = \tilde{\mathbf{Y}} v_l = \sum_{k=1}^d (v_l)_k y_{j_k}$$

where $\|v_l\|_\infty \leq 1$. Thus we obtain for all $l = 1, \dots, n$

$$\begin{aligned} \left\| (\mathbf{R} - \tilde{\mathbf{R}}) y_l \right\|_2 &= \left\| (\mathbf{R} - \tilde{\mathbf{R}}) \sum_{k=1}^d (v_l)_k y_{j_k} \right\|_2 \\ &\leq \sum_{k=1}^d |(v_l)_k| \left\| (\mathbf{R} - \tilde{\mathbf{R}}) y_{j_k} \right\|_2 \\ &\leq \sum_{k=1}^d \left\| (\mathbf{R} - \tilde{\mathbf{R}}) y_{j_k} \right\|_2 \\ &\leq \sqrt{d} (\tilde{\delta} + \delta). \end{aligned}$$

□

The next theorem is critical to the correctness of algorithm 1. If $IRMSD(S, \tilde{S}) \leq \epsilon$ for suitably small ϵ , it shows that the permutation π that is calculated in line 14 is equal to the globally optimal permutation π^* for the indices i_1, \dots, i_d that fulfill $\pi_{i_k}^* = j_k$. As the algorithm tests *all* index combinations i_1, \dots, i_d , one of them will yield the globally optimal permutation π^* .

Theorem 3. *Let $S = (\mathbf{x}, \mathbf{e})$ and $\tilde{S} = (\tilde{\mathbf{x}}, \tilde{\mathbf{e}})$ be two particle systems such that $IRMSD(S, \tilde{S}) \leq \epsilon$. We denote by n the number of particles in the systems and by d their dimensionality. Thus $\mathbf{x} = (x_1, \dots, x_n)$ consists of n d -dimensional points $x_i \in \mathbb{R}^d$ (similar for $\tilde{\mathbf{x}}$). By $\mathbf{R}^* \in \mathbb{O}_d$ and $\pi^* \in \mathbb{S}_n$ we denote the optimal orthogonal matrix and the optimal permutation in the calculation of the $IRMSD$ (see equation 2).*

Now assume that $\tilde{\mathbf{x}} = (\tilde{x}_1, \dots, \tilde{x}_n)$ fulfils the assumptions in theorem 1 and that j_1, \dots, j_d are the corresponding indices that maximise equation 6. Define the d indices i_1, \dots, i_k implicitly by $\pi_{i_k}^ = j_k$ ($\forall k = 1, \dots, d$) and $\mathbf{R} \in \mathbb{O}_d$ by*

$$\mathbf{R} = \arg \min_{\mathbf{R} \in \mathbb{O}_d} \sum_{k=1}^d \|x_{i_k} - \mathbf{R} \tilde{x}_{j_k}\|_2^2. \quad (15)$$

Let $\mu \in \mathbb{R}$ be the minimal particle distance in \tilde{S} , i.e.

$$\mu = \min_{i \neq j} \|\tilde{x}_i - \tilde{x}_j\|_2. \quad (16)$$

If $\epsilon < \frac{\mu}{2\sqrt{1+4d}}$, then π^ is equal to the permutation π that is defined by*

$$\begin{aligned} \pi_{i_k} &= j_k & \forall k = 1, \dots, d \\ \pi_k &= \arg \min_{l: e_k = \tilde{e}_l} \|x_k - \mathbf{R} \tilde{x}_l\|_2, & \forall k \notin \{i_1, \dots, i_d\}. \end{aligned} \quad (17)$$

Proof. By definition, $\pi_{i_k}^* = \pi_{i_k}$ for all $k = 1, \dots, d$. Thus it remains to show that $\pi_k^* = \pi_k$ for all $k \notin \{i_1, \dots, i_d\}$. To do this we define

$$\delta = \sqrt{\sum_{k=1}^d \|x_{i_k} - \mathbf{R}\tilde{x}_{j_k}\|_2^2} \quad (18)$$

and

$$\tilde{\delta} = \sqrt{\sum_{k=1}^d \|x_{i_k} - \mathbf{R}^*\tilde{x}_{j_k}\|_2^2}. \quad (19)$$

Due to the definition of \mathbf{R} we have $\delta \leq \tilde{\delta} \leq \epsilon$. Using theorem 2, we obtain

$$\|(\mathbf{R} - \mathbf{R}^*)\tilde{x}_k\|_2 \leq \sqrt{d}(\delta + \tilde{\delta}) \leq 2\sqrt{d}\tilde{\delta} \quad (20)$$

for all $k = 1, \dots, n$. For any $k \notin \{i_1, \dots, i_d\}$ we can write

$$\begin{aligned} \epsilon^2 &\geq \text{IRMSD}(S, \tilde{S})^2 = \sum_{l=1}^n \|x_l - \mathbf{R}^*\tilde{x}_{\pi_l^*}\|_2^2 \\ &= \sum_{l=1}^d \|x_{i_l} - \mathbf{R}^*\tilde{x}_{j_l}\|_2^2 + \sum_{\substack{l=1 \\ l \notin \{i_1, \dots, i_d\}}}^n \|x_l - \mathbf{R}^*\tilde{x}_{\pi_l^*}\|_2^2 \\ &= \tilde{\delta}^2 + \sum_{\substack{l=1 \\ l \notin \{i_1, \dots, i_d\}}}^n \|x_l - \mathbf{R}^*\tilde{x}_{\pi_l^*}\|_2^2 \\ &\geq \tilde{\delta}^2 + \|x_k - \mathbf{R}^*\tilde{x}_{\pi_k^*}\|_2^2. \end{aligned}$$

and thus obtain:

$$\|x_k - \mathbf{R}^*\tilde{x}_{\pi_k^*}\|_2 \leq \sqrt{\epsilon^2 - \tilde{\delta}^2}. \quad (21)$$

Putting all things together we obtain for $k \notin \{i_1, \dots, i_d\}$:

$$\begin{aligned} \|x_k - \mathbf{R}\tilde{x}_{\pi_k^*}\|_2 &= \|x_k + \mathbf{R}^*\tilde{x}_{\pi_k^*} - \mathbf{R}^*\tilde{x}_{\pi_k^*} - \mathbf{R}\tilde{x}_{\pi_k^*}\|_2 \\ &\leq \|x_k - \mathbf{R}^*\tilde{x}_{\pi_k^*}\|_2 + \|(\mathbf{R} - \mathbf{R}^*)\tilde{x}_{\pi_k^*}\|_2 \\ &\leq \sqrt{\epsilon^2 - \tilde{\delta}^2} + 2\sqrt{d}\tilde{\delta} \\ &\leq \sqrt{1 + 4d}\epsilon, \end{aligned} \quad (22)$$

where the final inequality can be obtained by maximising $\sqrt{\epsilon^2 - \tilde{\delta}^2} + 2\sqrt{d}\tilde{\delta}$ with respect to $\tilde{\delta}$. Equation 22 shows that $\mathbf{R}\tilde{x}_{\pi_k^*}$ is located in a sphere of radius $\sqrt{1 + 4d}\epsilon$ around x_k . As $\epsilon < \frac{\mu}{2\sqrt{1+4d}}$, $\tilde{x}_{\pi_k^*}$ is the only point in \tilde{x} that lies inside this radius and thus π_k^* minimises equation 17. \square

The following lemma and the subsequent theorem are needed by theorem 5 which is needed to prove the complexity of algorithm 1.

Lemma 1. (Taken from [20, 21]) Let $\mathbf{A} \in \mathbb{R}^{d \times d}$ be a square matrix and denote by $\mathbf{A}(\mathbf{i})$ the matrix \mathbf{A} with its i -th column removed. Then some index $k \in \{1, \dots, d\}$ exist such that

$$\|\mathbf{A} - \mathbf{A}(\mathbf{k})\mathbf{A}(\mathbf{k})^+\mathbf{A}\|_F \leq \sqrt{d}\sigma_d(\mathbf{A}).$$

Here, $\sigma_d(\mathbf{A})$ denotes the d -th largest (i.e. smallest) singular value of \mathbf{A} and $\mathbf{A}(\mathbf{k})^+$ is the Moore-Penrose pseudo-inverse of $\mathbf{A}(\mathbf{k})$.

Theorem 4. Let $\mathbf{A} \in \mathbb{R}^{d \times d}$ be non-singular and $k \in \{1, \dots, d\}$ be an index such that

$$\|\mathbf{A} - \mathbf{A}(\mathbf{k})\mathbf{A}(\mathbf{k})^+\mathbf{A}\|_F \leq \sqrt{d}\sigma_d(\mathbf{A})$$

(due to lemma 1 at least one such index exists). Then for each orthogonal matrix $\mathbf{U} \in \mathbb{O}_d$ at least one of the following inequalities holds

$$\|\mathbf{A}_{*,k} - \mathbf{U}\mathbf{A}_{*,k}\|_2 \leq (1 + \sqrt{2})\sqrt{d}\|\mathbf{U}\mathbf{A}(\mathbf{k}) - \mathbf{A}(\mathbf{k})\|_F \quad (23)$$

$$\|2\mathbf{A}(\mathbf{k})\mathbf{A}(\mathbf{k})^+\mathbf{A}_{*,k} - \mathbf{A}_{*,k} - \mathbf{U}\mathbf{A}_{*,k}\|_2 \leq (1 + \sqrt{2})\sqrt{d}\|\mathbf{U}\mathbf{A}(\mathbf{k}) - \mathbf{A}(\mathbf{k})\|_F. \quad (24)$$

Proof. To simplify the notation, it is assumed w.l.o.g. that $k = d$. As \mathbf{A} is non-singular, its d -th column $\mathbf{A}_{*,d}$ can also be written as

$$\mathbf{A}_{*,d} = \mathbf{A}(\mathbf{d}) \underbrace{\mathbf{A}(\mathbf{d})^+\mathbf{A}_{*,d}}_{=: \mathbf{v}} + \mathbf{c}$$

where \mathbf{c} is from the (one-dimensional) nullspace of $\mathbf{A}(\mathbf{d})^T$. Setting $\delta(\mathbf{U}) := \mathbf{U}\mathbf{A}(\mathbf{k}) - \mathbf{A}(\mathbf{k})$ immediately yields

$$\mathbf{U}\mathbf{A}(\mathbf{d})\mathbf{v} - \mathbf{A}(\mathbf{d})\mathbf{v} = \delta(\mathbf{U})\mathbf{v}$$

and thus

$$\|\mathbf{U}\mathbf{A}(\mathbf{d})\mathbf{v} - \mathbf{A}(\mathbf{d})\mathbf{v}\|_2 \leq \|\delta(\mathbf{U})\|_F \|\mathbf{v}\|_2.$$

The norm of \mathbf{v} can be bounded from above as follows (e_d is the d -th unit vector)

$$\begin{aligned} \|e_d - [\mathbf{I} \ 0]^T \mathbf{v}\|_2 &= \|e_d - \mathbf{A}^{-1}\mathbf{A}(\mathbf{d})\mathbf{A}(\mathbf{d})^+\mathbf{A}e_d\|_2 \\ &= \|\mathbf{A}^{-1}(\mathbf{A}e_d - \mathbf{A}(\mathbf{d})\mathbf{A}(\mathbf{d})^+\mathbf{A}e_d)\|_2 \\ &\leq \|\mathbf{A}^{-1}\|_2 \|\mathbf{A} - \mathbf{A}(\mathbf{d})\mathbf{A}(\mathbf{d})^+\mathbf{A}\|_F \|e_d\|_2 \\ &\leq \frac{1}{\sigma_d(\mathbf{A})} \sqrt{d}\sigma_d(\mathbf{A}) = \sqrt{d} \\ \Rightarrow \|e_d - [\mathbf{I} \ 0]^T \mathbf{v}\|_2^2 &= \left\| \begin{pmatrix} \mathbf{v} \\ 1 \end{pmatrix} \right\|_2^2 \leq d \Rightarrow \|\mathbf{v}\|_2^2 \leq d - 1. \end{aligned}$$

The next step is to prove a similar inequality for $\|\mathbf{c} - \mathbf{U}\mathbf{c}\|_2$. Due to the properties of orthogonal matrices one can easily verify that $\tilde{\mathbf{c}} := \mathbf{U}\mathbf{c}$ must have the same Euclidean norm as \mathbf{c} and must be in the nullspace of $(\mathbf{U}\mathbf{A}(\mathbf{d}))^T$. Therefore $\tilde{\mathbf{c}}$ must fulfil

$$(\mathbf{U}\mathbf{A}(\mathbf{d}))^T \tilde{\mathbf{c}} = (\mathbf{A}(\mathbf{d}) + \delta(\mathbf{U}))^T \tilde{\mathbf{c}} = 0 \quad (25)$$

$$\tilde{\mathbf{c}}^T \tilde{\mathbf{c}} = \mathbf{c}^T \mathbf{c}. \quad (26)$$

Using once again the fact that $\mathbf{A}(\mathbf{d})$ and \mathbf{c} span the whole \mathbb{R}^d , $\tilde{\mathbf{c}}$ can be written as $\tilde{\mathbf{c}} = \mathbf{A}(\mathbf{d})\mathbf{w} + a\mathbf{c}$ for some (yet to be determined) $\mathbf{w} \in \mathbb{R}^{d-1}$ and $a \in \mathbb{R}$. Due to equation (25), $\tilde{\mathbf{c}}$ must fulfil

$$\mathbf{A}(\mathbf{d})^T \tilde{\mathbf{c}} = -\delta(\mathbf{U})^T \tilde{\mathbf{c}}$$

and thus

$$\mathbf{A}(\mathbf{d})^T (\mathbf{A}(\mathbf{d})\mathbf{w} + a\mathbf{c}) = \mathbf{A}(\mathbf{d})^T \mathbf{A}(\mathbf{d})\mathbf{w} = -\delta(\mathbf{U})^T \tilde{\mathbf{c}}.$$

As $\mathbf{A}(\mathbf{d})^T \mathbf{A}(\mathbf{d})$ is invertible, \mathbf{w} fulfils

$$\mathbf{w} = -(\mathbf{A}(\mathbf{d})^T \mathbf{A}(\mathbf{d}))^{-1} \delta(\mathbf{U})^T \tilde{\mathbf{c}}$$

and thus (using $\|\tilde{\mathbf{c}}\|_2 = \|\mathbf{c}\|_2$)

$$\begin{aligned} \|\mathbf{A}(\mathbf{d})\mathbf{w}\|_2 &= \left\| -\mathbf{A}(\mathbf{d})(\mathbf{A}(\mathbf{d})^T \mathbf{A}(\mathbf{d}))^{-1} \delta(\mathbf{U})^T \tilde{\mathbf{c}} \right\|_2 = \left\| -\mathbf{A}(\mathbf{d})^{\mathbf{T}^+} \delta(\mathbf{U})^T \tilde{\mathbf{c}} \right\|_2 \\ &\leq \left\| \mathbf{A}(\mathbf{d})^{\mathbf{T}^+} \right\|_2 \left\| \delta(\mathbf{U})^T \right\|_F \|\tilde{\mathbf{c}}\|_2 = \|\mathbf{A}(\mathbf{d})^+\|_2 \|\delta(\mathbf{U})\|_F \|\mathbf{c}\|_2. \end{aligned} \quad (27)$$

Once again using $\|\mathbf{c}\|_2 = \|\tilde{\mathbf{c}}\|_2$ one obtains

$$\begin{aligned} \mathbf{c}^T \mathbf{c} &= \mathbf{w}^T \mathbf{A}(\mathbf{d})^T \mathbf{A}(\mathbf{d})\mathbf{w} + a^2 \mathbf{c}^T \mathbf{c} + 2a\mathbf{w}^T \mathbf{A}(\mathbf{d})^T \mathbf{c} \\ &= \|\mathbf{A}(\mathbf{d})\mathbf{w}\|_2^2 + a^2 \mathbf{c}^T \mathbf{c} \end{aligned}$$

which is a quadratic equation with respect to a and thus has two solutions a_+ and a_- , given by

$$a_{\pm} = \pm \sqrt{1 - \frac{\|\mathbf{A}(\mathbf{d})\mathbf{w}\|_2^2}{\mathbf{c}^T \mathbf{c}}}.$$

As $\|\mathbf{A}(\mathbf{d})\mathbf{w}\|_2$ is limited from above (see equation (27)), a_+ fulfils

$$a_+ = \sqrt{1 - \frac{\|\mathbf{A}(\mathbf{d})\mathbf{w}\|_2^2}{\mathbf{c}^T \mathbf{c}}} \geq 1 - \|\mathbf{A}(\mathbf{d})^+\|_2^2 \|\delta(\mathbf{U})\|_F^2$$

and $a_- \leq -\left(1 - \|\mathbf{A}(\mathbf{d})^+\|_2^2 \|\delta(\mathbf{U})\|_F^2\right)$. Now $\tilde{\mathbf{c}}$ is equal to either $\mathbf{A}(\mathbf{d})\mathbf{w} + a_+\mathbf{c}$ or

$\mathbf{A}(\mathbf{d})\mathbf{w} + a_-\mathbf{c}$. In the first case, $\|\tilde{\mathbf{c}} - \mathbf{c}\|_2^2$ fulfils

$$\begin{aligned}
\|\tilde{\mathbf{c}} - \mathbf{c}\|_2^2 &= 2\mathbf{c}^T\mathbf{c} - \underbrace{\mathbf{c}^T\mathbf{A}(\mathbf{d})\mathbf{w}}_{=0} - 2a_+\mathbf{c}^T\mathbf{c} = 2\mathbf{c}^T\mathbf{c}(1 - a_+) \leq 2\mathbf{c}^T\mathbf{c} \|\mathbf{A}(\mathbf{d})^+\|_2^2 \|\delta(\mathbf{U})\|_F^2 \\
&= 2 \|\mathbf{A}(\mathbf{d})^+\|_2^2 \|\delta(\mathbf{U})\|_F^2 \|\mathbf{c}\|_2^2 \\
&= 2 \|\mathbf{A}(\mathbf{d})^+\|_2^2 \|\delta(\mathbf{U})\|_F^2 \|\mathbf{A}_{*,d} - \mathbf{A}(\mathbf{d})\mathbf{A}(\mathbf{d})^+\mathbf{A}_{*,d}\|_2^2 \\
&\leq 2 \|\mathbf{A}(\mathbf{d})^+\|_2^2 \|\delta(\mathbf{U})\|_F^2 \|\mathbf{A} - \mathbf{A}(\mathbf{d})\mathbf{A}(\mathbf{d})^+\mathbf{A}\|_F^2 \\
&\leq 2 \frac{1}{\sigma_{d-1}^2(\mathbf{A}(\mathbf{d}))} \|\delta(\mathbf{U})\|_F^2 d\sigma_d^2(\mathbf{A}) \\
&\leq 2d \|\delta(\mathbf{U})\|_F^2
\end{aligned}$$

and thus equation (23) holds

$$\begin{aligned}
\|\mathbf{A}(\mathbf{d})\mathbf{v} + \mathbf{c} - \mathbf{U}(\mathbf{A}(\mathbf{d})\mathbf{v} + \mathbf{c})\|_2 &= \|-\delta(\mathbf{U})\mathbf{v} + \mathbf{c} - \tilde{\mathbf{c}}\|_2 \leq \|\delta(\mathbf{U})\mathbf{v}\|_2 + \|\mathbf{c} - \tilde{\mathbf{c}}\|_2 \\
&\leq \|\delta(\mathbf{U})\|_F \sqrt{d} + \sqrt{2d} \|\delta(\mathbf{U})\|_F \\
&= (1 + \sqrt{2})\sqrt{d} \|\delta(\mathbf{U})\|_F.
\end{aligned}$$

If $\tilde{\mathbf{c}} = \mathbf{A}(\mathbf{d})\mathbf{w} + a_-\mathbf{c}$, the second inequality can be derived using $\mathbf{A}(\mathbf{d})\mathbf{v} - \mathbf{c}$ instead of $\mathbf{A}(\mathbf{d})\mathbf{v} + \mathbf{c}$. \square

Theorem 5. Let (x_1, \dots, x_n) be n d -dimensional points ($x_i \in \mathbb{R}^d$) such that

$$\|x_i - x_j\|_2 \geq \mu, \quad i \neq j$$

for some $\mu > 0$. Furthermore let $\tilde{x}_1, \dots, \tilde{x}_d$ be d d -dimensional points ($\tilde{x}_i \in \mathbb{R}^d$) that are linearly independent. Then the magnitude of the set

$$I = \left\{ i \in \{1, \dots, n\}^d : (i_j \neq i_k \forall j \neq k) \wedge \left(\exists \mathbf{R} \in \mathbb{O}_d : \sum_{l=1}^d \|x_{i_l} - \mathbf{R}\tilde{x}_l\|_2^2 \leq \epsilon^2 \right) \right\}$$

is of order $O(2.415^d n^{d-1})$ if $\epsilon < \frac{\mu}{2\sqrt{1+4d}}$.

Proof. To begin with, let $\tilde{\mathbf{X}} = [\tilde{x}_1, \dots, \tilde{x}_d]$ be the matrix that has the vectors \tilde{x}_i as columns. Then $\tilde{\mathbf{X}}$ fulfils all conditions of lemma 1 and therefore some index k exists such that

$$\left\| \tilde{\mathbf{X}} - \tilde{\mathbf{X}}(\mathbf{k})\tilde{\mathbf{X}}(\mathbf{k})^+\tilde{\mathbf{X}} \right\|_F \leq \sqrt{d}\sigma_d(\tilde{\mathbf{X}}).$$

W.l.o.g. it is assumed here that $k = d$, otherwise one can simply permute the \tilde{x}_i and x_i . Then every $i \in I$ can be written as $i = (j, l)$ where $j \in \{1, \dots, n\}^{d-1}$ and $l \in \{1, \dots, n\}$. If $(j, l) \in I$, j must fulfil

$$(j_m \neq j_p \forall m \neq p) \wedge \left(\exists \mathbf{R} \in \mathbb{O}_d : \sum_{m=1}^{d-1} \|x_{j_m} - \mathbf{R}\tilde{x}_m\|_2^2 \leq \epsilon^2 \right).$$

Due to the condition that all entries of j must be distinct, there are only up to $\binom{n}{d-1} = O(n^{d-1})$ possible tuples j . It is now shown that for each such j , no more than $2 \cdot 2.415^d$ possible values \tilde{l} exist such that $(j, \tilde{l}) \in I$.

To prove this, it can easily be observed that for $i = (j, l) \in I$ the relation

$$\underbrace{\left\{ \mathbf{R} \in \mathbb{O}_d : \sum_{m=1}^{d-1} \|x_{j_m} - \mathbf{R}\tilde{x}_m\|_2^2 \leq \epsilon^2 \right\}}_{=\mathcal{R}_j} \supseteq \left\{ \mathbf{R} \in \mathbb{O}_d : \sum_{m=1}^{d-1} \|x_{j_m} - \mathbf{R}\tilde{x}_m\|_2^2 + \|x_l - \mathbf{R}\tilde{x}_d\|_2^2 \leq \epsilon^2 \right\}$$

holds. Furthermore, all $\mathbf{R}, \tilde{\mathbf{R}} \in \mathcal{R}_j$ fulfil

$$\left\| \mathbf{R}\tilde{\mathbf{X}}(\mathbf{d}) - \tilde{\mathbf{R}}\tilde{\mathbf{X}}(\mathbf{d}) \right\|_F \leq 2\epsilon. \quad (28)$$

Therefore, choosing an arbitrary $\mathbf{R} \in \mathcal{R}_j$ and setting $\mathbf{A} = \mathbf{R}\tilde{\mathbf{X}}$ in theorem 4 yields two vectors $\mathbf{y} \in \mathbb{R}^d$ and $\tilde{\mathbf{y}} \in \mathbb{R}^d$ such that $\forall \tilde{\mathbf{R}} \in \mathcal{R}_j$ either \mathbf{y} or $\tilde{\mathbf{y}}$ fulfil

$$\begin{aligned} \left\| \mathbf{y} - \tilde{\mathbf{R}}\tilde{\mathbf{X}}_{*,d} \right\|_2 &= \left\| \mathbf{y} - \tilde{\mathbf{R}}\mathbf{R}^T(\mathbf{R}\tilde{\mathbf{X}}_{*,d}) \right\|_2 \leq (1 + \sqrt{2})\sqrt{d} \left\| \mathbf{R}\tilde{\mathbf{X}}(d) - \tilde{\mathbf{R}}\mathbf{R}^T(\mathbf{R}\tilde{\mathbf{X}}(\mathbf{d})) \right\|_F \\ &= (1 + \sqrt{2})\sqrt{d} \left\| \mathbf{R}\tilde{\mathbf{X}}(\mathbf{d}) - \tilde{\mathbf{R}}\tilde{\mathbf{X}}(\mathbf{d}) \right\|_F. \end{aligned}$$

Due to equation (28) this leads to either

$$\left\| \mathbf{y} - \tilde{\mathbf{R}}\tilde{x}_d \right\|_2 \leq 2(1 + \sqrt{2})\sqrt{d}\epsilon$$

or

$$\left\| \tilde{\mathbf{y}} - \tilde{\mathbf{R}}\tilde{x}_d \right\|_2 \leq 2(1 + \sqrt{2})\sqrt{d}\epsilon$$

Due to these inequalities, each feasible $\tilde{\mathbf{R}} \in \mathcal{R}_j$ transforms \tilde{x}_d into a sphere of radius $2(1 + \sqrt{2})\sqrt{d}\epsilon$ around either \mathbf{y} or $\tilde{\mathbf{y}}$. Thus, the corresponding x_d must also lie in one of these spheres. As the x_i were assumed to fulfil $\|x_i - x_j\|_2 \geq \mu$, only a limited number of x_i -s can lie in these spheres. As the diameter of each sphere is no more than

$$\frac{2 \cdot 2(1 + \sqrt{2})\sqrt{d}\epsilon}{\mu} < \frac{2 \cdot 2(1 + \sqrt{2})\sqrt{d}\epsilon}{2\sqrt{1 + 4d}\epsilon} = \frac{2(1 + \sqrt{2})\sqrt{d}}{\sqrt{d}\sqrt{\frac{1}{d} + 4}} \leq \frac{2 + 2\sqrt{2}}{\sqrt{4}} \leq 2.415$$

times larger than μ – and thus independent of n – the maximal number of points x_i that fit in such a sphere cannot be larger than 2.415^d .

Thus if $(j, l) \in I$, for each j there are no more than $2 \cdot 2.415^d$ possible $\tilde{l} \in \{1, \dots, n\}$ such that (j, \tilde{l}) is also in I . \square

6.2 Go-Permdist lower bound

The Go-Permdist algorithm in [9] tries to find the optimal *IRMSD* by decomposing the space of all rotations into *rotation cubes* $C(\mathbf{v}, \theta_B) = \{\mathbf{r} \in [-\pi, \pi]^3 : \|\mathbf{r} - \mathbf{v}\|_\infty \leq \theta_B\}$. Each vector \mathbf{r} in a rotation cube represents a rotation of angle $\|\mathbf{r}\|_2$ around the rotation axis $\mathbf{r}/\|\mathbf{r}\|_2$. For simplicity we will write $\mathbf{r}(\mathbf{x})$ to denote a vector \mathbf{x} that is rotated by \mathbf{r} . In order to work, the Go-Permdist algorithm needs a lower bound $LB(\mathbf{v}, \theta_B)$ that depends only on \mathbf{v} and θ_B such that

$$LB(\mathbf{v}, \theta_B) \leq \cos(\angle(\mathbf{v}(\mathbf{x}), \mathbf{r}(\mathbf{x}))), \quad \forall \mathbf{r} \in C(\mathbf{v}, \theta_B), \mathbf{x} \in \mathbb{R}^3. \quad (29)$$

In equation 19 of the cited paper such a lower bound is derived that unfortunately does not hold true in all cases. As a simple counter example $\mathbf{v} = (-0.25\pi, 0.25\pi, 0.25\pi)$, $\mathbf{r} = (-0.48\pi, 0.02\pi, 0)$, $\mathbf{x} = (0.12\pi, -0.14\pi, 0)$ and $\theta_B = 0.5\pi$ can be chosen. As the problem seems to be just a missing factor $\sqrt{3}$, adding it to equation 19 in the original paper results in the corrected lower bound

$$LB(\mathbf{v}, \theta_B) = \cos\left(\min\left[\pi, \sqrt{3}\frac{\theta_B}{2}\right]\right). \quad (30)$$

Acknowledgement

This work was funded in parts by the Bundesministerium für Bildung und Forschung (BMBF) as a part of the Eurostars project E!9389 MultiModel.

The main algorithm and all related proofs originate from the PhD thesis of one of the authors [22].

Conflict of interest disclosure

The *Fraunhofer Institute for Algorithms and Scientific Computing* offers commercial software products that include the described comparison procedure.

References

- [1] Michael C. Shaughnessy and Reese E. Jones. Efficient use of an adapting database of ab initio calculations to generate accurate Newtonian dynamics. *Journal of Chemical Theory and Computation*, 12(2):664–675, 2016.
- [2] Fedwa El-Mellouhi, Normand Mousseau, and Laurent J. Lewis. Kinetic activation-relaxation technique: an off-lattice self-learning kinetic Monte Carlo algorithm. *Phys. Rev. B*, 78:153202, 2008.
- [3] Dhrubajit Konwar, Vijesh J. Bhute, and Abhijit Chatterjee. An off-lattice, self-learning kinetic Monte Carlo method using local environments. *The Journal of Chemical Physics*, 135(17):174103, 2011.

- [4] Ali Sadeghi, S. Alireza Ghasemi, Bastian Schaefer, Stephan Mohr, Markus A. Lill, and Stefan Goedecker. Metrics for measuring distances in configuration spaces. *The Journal of Chemical Physics*, 139(18):184118, 2013.
- [5] Hongdong Li and Richard Hartley. The 3D-3D registration problem revisited. In *2007 IEEE 11th International Conference on Computer Vision*, pages 1–8, 2007.
- [6] Paul J. Besl and Neil D. McKay. A method for registration of 3-D shapes. *IEEE Transactions on Pattern Analysis and Machine Intelligence*, 14(2):239–256, 1992.
- [7] Steven Gold, Anand Rangarajan, Chien-Ping Lu, Suguna Pappu, and Eric Mjølness. New algorithms for 2D and 3D point matching: pose estimation and correspondence. *Pattern Recognition*, 31(8):1019 – 1031, 1998.
- [8] Jiaolong Yang, Hongdong Li, and Yunde Jia. Go-ICP: solving 3D registration efficiently and globally optimally. In *2013 IEEE International Conference on Computer Vision*, pages 1457–1464, 2013.
- [9] Matthew Griffiths, Samuel P. Niblett, and David J. Wales. Optimal alignment of structures for finite and periodic systems. *Journal of Chemical Theory and Computation*, 13(10):4914–4931, 2017.
- [10] Wolfgang Kabsch. A solution for the best rotation to relate two sets of vectors. *Acta Crystallographica Section A*, 32(5):922–923, 1976.
- [11] Jon L. Bentley, Donald F. Stanat, and E. Hollins Williams. The complexity of finding fixed-radius near neighbors. *Information Processing Letters*, 6(6):209 – 212, 1977.
- [12] Synopsys QuantumATK 2019.12. <https://www.synopsys.com/silicon/quantumatk.html>.
- [13] Søren Smidstrup, Troels Markussen, Pieter Vancraeyveld, Jess Wellendorff, Julian Schneider, Tue Gunst, Brecht Verstichel, Daniele Stradi, Petr A Khomyakov, Ulrik G Vej-Hansen, Maeng-Eun Lee, Samuel T Chill, Filip Rasmussen, Gabriele Penazzi, Fabiano Corsetti, Ari Ojanperä, Kristian Jensen, Mattias L N Palsgaard, Umberto Martinez, Anders Blom, Mads Brandbyge, and Kurt Stokbro. QuantumATK: an integrated platform of electronic and atomic-scale modelling tools. *Journal of Physics: Condensed Matter*, 32(1):015901, 2019.
- [14] libAtoms.org data repository. <http://www.libatoms.org/Home/DataRepository>.
- [15] Albert P. Bartók, James Kermode, Noam Bernstein, and Gábor Csányi. Machine learning a general-purpose interatomic potential for silicon. *Phys. Rev. X*, 8:041048, 2018.
- [16] Evguenii A Rakhmanov, Edward B Saff, and YM Zhou. Minimal discrete energy on the sphere. *Mathematical Research Letters*, 1(6):647–662, 1994.

- [17] Go-ICP algorithm, git commit 937f114590f7df8b003d05f594b55527e230fef0. <https://github.com/yangjiaolong/Go-ICP>.
- [18] Go-Permdist algorithm, git commit 4db8e51a4719a405cc2db5475d2cef5453da68a3. <https://github.com/matthewghgriffiths/fastoverlap>.
- [19] Aleksandr Mikhalev and Ivan Oseledets. Rectangular maximum-volume submatrices and their applications. *arXiv e-prints*, 2015.
- [20] Alice Cortinovis and Daniel Kressner. Low-rank approximation in the Frobenius norm by column and row subset selection. *arXiv e-prints*, 2019.
- [21] Amit Deshpande, Luis Rademacher, Santosh Vempala, and Grant Wang. Matrix approximation and projective clustering via volume sampling. In *Proceedings of the Seventeenth Annual ACM-SIAM Symposium on Discrete Algorithm*, SODA '06, page 1117–1126, USA, 2006. Society for Industrial and Applied Mathematics.
- [22] Johannes Bulin. *Long-timescale atomistic simulations*. PhD thesis, Rheinische Friedrich-Wilhelms-Universität Bonn, 2021.